Journal of Building Engineering 43 (2021) 102908

Contents lists available at ScienceDirect

Journal of Building Engineering

journal homepage: http://www.elsevier.com/locate/jobe

A structural performance-based environmental impact assessment framework for natural hazard loads

Rafael A. Salgado *, Serhan Guner

Department of Civil and Environmental Engineering, University of Toledo, Toledo, OH, 43607, USA

ARTICLE INFO

Keywords:
Life cycle assessment
Multidisciplinary framework
Natural hazard
Nonlinear modeling
Resilience

ABSTRACT

The decision-making process of planning a sustainable and resilient community may often encounter the availability of different building design alternatives that can make use of different structural solutions, which inevitably translate into different environmental impacts and structural performances to natural hazards. To reveal the trade-offs among different design alternatives and effectively support decision-making, the differences in environmental and structural performance must be simultaneously accounted so that the environmental benefits provided by an eco-friendlier alternative do not jeopardize resilience in the form of natural-hazard structural performance. The objective of this study is to take the first step in creating a multidisciplinary framework that combines PBD and LCA to enable the direct comparison of the structural performance-based environmental impacts of different building alternatives. Using a developed performance normalization index, the framework normalizes the structural performance of the building alternatives investigated to enable a direct quantitative comparison of their environmental impacts. The framework can help decision makers select the most suitable building alternative for balanced structural performance to natural hazard loads and environmental impacts. For demonstration purposes, the framework is applied to compare two seven-story building alternatives made from cross laminated timber and reinforced concrete materials in a tsunami-prone region. The results of the case study indicated that the normalized environmental impacts of the RC building were lower than the CLT building for most limit states considered, which may not have been evident without the proposed framework.

1. Introduction

One of the climate change effects accentuated by the degradation of the environment is the increase in frequency and magnitude of natural hazard events such as earthquakes, tsunamis, hurricanes, floods, etc. The damage caused by these events (in the form of economic, downtime, social disruption, loss of lives, etc.) has been rapidly increasing due to the urbanization of vulnerable areas. As a result, urban centers are seeking ways of creating resilient communities that can withstand extreme situations, such as natural hazard events, while remaining functional and in a safe state [1]. The built environment of these communities is at the center of this move towards resiliency because it dictates their structural performance and has the potential to significantly reduce emissions associated with greenhouse effects and climate change [2].

Regarding the structural performance of building structures, one of the most promising tools used to reduce the damage and losses resulting from natural hazards is the performance-based design (PBD) methodology [3]. PBD accounts for the inherent uncertainties and risks associated with natural hazards events and building construction by employing advanced structural analysis and probabilistic methods to predict a structure's response more reliably. Compared to traditional prescriptive design where the building must conform to a series of code requirements that results in a hard-to-quantify performance, PBD evaluates the building to demonstrate that an explicitly defined desired performance can be achieved [4]. The performance assessment provided by the PBD methodology has made it a crucial tool in the planning communities' structural resilience. Recent years have seen the use and expansion of PBD for the study of several aspects of buildings. Since PBD relies on advanced structural analysis methods, the efficiency of different analysis methods ranging from simple static methods to advanced dynamic analyses has been investigated [5–16]. For many years, earthquakes were the focus of PBD investigations [17–28] but, more recently, other natural hazards and multi-hazard events have also been studied [29–42].

* Corresponding author.
E-mail addresses: rafael.salgado@rockets.utoledo.edu (R.A. Salgado), serhan.guner@utoledo.edu (S. Guner).

https://doi.org/10.1016/j.jobe.2021.102908
Received 4 October 2020; Received in revised form 13 June 2021; Accepted 16 June 2021
Available online 24 June 2021
2352-7102/© 2021 Elsevier Ltd. All rights reserved.

Regarding their environmental impacts, the building industry is one of the major exploiters of the environment in the form of nonrenewable resource depletion, waste generation, energy consumption, and CO_2 emissions, resulting in as much as 40% of the world material consumption and 30–40% of the total energy demand and greenhouse gas emissions [2,43,44]. The life cycle assessment (LCA) framework [45,46] is a valuable tool for evaluating the environmental impacts of products, systems, or processes while considering its entire life cycle [47]. Many different aspects of building structures have been studied using the LCA framework. Previous LCA studies have demonstrated that the majority of buildings' impacts occur in the material extraction and operational phases [43,48–51], which fostered the comparative investigation of the environmental impacts of different building alternatives such as RC compared to structural steel buildings [52–55], RC compared to wood buildings [56,57], the use of precast concrete alternatives [58], energy consumption of buildings with standard or green roofs [59,60], impacts of low-energy-use [61] and green [62] buildings, and impacts of efficient insulation techniques [63].

The desire to move towards resilient and sustainable communities has motivated the integration of the performance-based design and life cycle assessment methodologies. This integration has the potential to assist in the decision-making process of selecting building designs that minimize economic losses, downtime, casualties, and environmental impacts due to natural hazard events while revealing trade-offs among design alternatives [48]. The LCA-PBD integration also allows for a more robust environmental analysis that incorporates the concepts of risk, performance, and probability inherited from the PBD methodology. Under this perspective, studies have combined LCA and PBD to calculate the environmental impacts associated with different structural performances of buildings [64–70]. In addition, retrofitting actions [47,71–73] and demolition waste [47,72,74,75] resultant from the damage caused by the extreme loads imposed by natural hazards have been incorporated in the holistic performance-based environmental impact of buildings.

The above examples illustrate how the PBD and LCA methodologies are, both separately and combined, powerful tools for the creation of sustainable and resilient communities of the future. The vast majority of the existing research, however, has focused on evaluating – or creating tools and methodologies to allow the evaluation – of the performance-based environmental impacts of isolated buildings (e.g., Refs. [2,48,71]). The decision-making process of planning a sustainable and resilient community may often encounter the availability of different building design alternatives – an important area that has received much less scientific attention. Different design alternatives can make use of different structural materials and solutions to their gravity and lateral force resisting systems, which inevitably translate into different environmental impacts and structural performances to natural hazards. Thus, to reveal the trade-offs among different design alternatives and effectively support decision-making, the differences in environmental and structural performance must be simultaneously accounted so that the environmental benefits provided by an eco-friendlier alternative do not jeopardize resilience in the form of natural-hazard structural performance.

The objective of this study is to take the first step in creating a multidisciplinary framework that combines PBD and LCA to enable the direct comparison of the structural performance-based environmental impacts of different building alternatives. The framework aims to provide a science-based methodology for revealing the trade-offs among different design alternatives and to effectively support decision-making by simultaneously accounting for their environmental impacts and structural performance to natural hazard loads. Using a developed performance normalization index, the framework normalizes the environmental impacts of each building alternative investigated based on their structural performance to enable a direct quantitative comparison. The framework can help better inform decision-makers when selecting the most suitable building alternative for balancing environmental impacts and structural performance to natural hazard loads. For demonstration purposes, the framework is applied to compare two seven-story building alternatives made from cross laminated timber and reinforced concrete materials in a tsunami-prone region.

2. Structural performance-based environmental impact assessment framework

The proposed framework stems from the need of being able to compare multiple building design alternatives through the calculation of an index that modifies their calculated environmental impacts based on the differences in structural performance. As an illustrative example, when comparing two design alternatives with similar environmental impacts, the framework aims to account for the detrimental effects of one of the alternatives having a weaker structural performance by calculating a higher index value that increases its environmental impacts. As a result, the framework presents environmental impacts for each investigated building alternative corrected – or normalized – to an equivalent structural performance, allowing a direct comparison analysis for decision-makers.

As one of the first steps towards the creation of a framework to account for the structural performance and environmental impacts of buildings, the authors have set the objective of making the first iteration of this framework as simple and practical as possible. To achieve that, the framework uses a discrete hazard analysis approach similar to the first-generation PBD procedures [76] rather than the rigorous probabilistic approach of PBD, as the completion of such process for a given building requires a very large amount of data gathering and computational work [7,8,77] and, as such, is not directly applicable to most ordinary structures from a practical perspective.

An overview of the framework proposed in this study is shown in Fig. 1. As for the PBD methodology [78], advanced computational modeling methods are also the foundation of the proposed framework. Con-

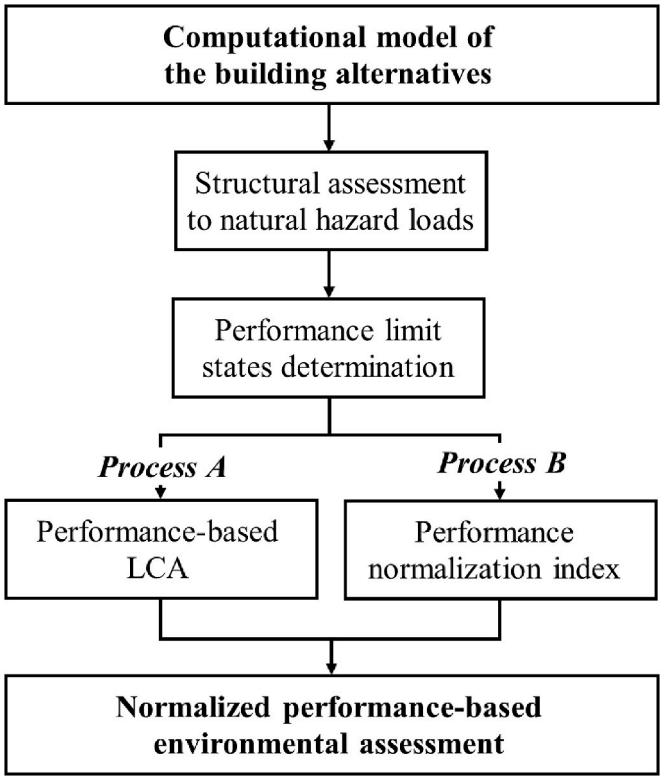

Fig. 1. Multidisciplinary framework for the combined structural and environmental assessment of buildings.

sequently, computational models of each building alternative investigated are first created and subjected to the expected natural hazard loads. The calculated structural response of each building alternative is then used to determine the thresholds for their expected damage levels in order to classify their performance to the natural hazard loads. These thresholds – or limit states – are used as the basis for two concurrent processes. In process A, a performance-based LCA analysis of each building alternative is performed including environmental impacts associated with identified post-natural hazard-induced damage building actions. This process is analogous to the PBD-LCA implementation vastly found in the available literature. In Process B, the difference between the calculated limit states of the investigated building design alternatives is used to calculate the Performance Normalization Index (PNI). Finally, the LCA results of Process A are modified by the PNIs calculated in Process B to obtain environmental impacts that are normalized to the investigated buildings' difference of structural performance. These normalized impacts are then used in the direct quantitative comparison of the building alternative's environmental impacts.

2.1. Computational model of the building alternatives

The proposed framework relies on the accurate characterization of the buildings' responses to predict their performance and damage characteristics. Under natural hazard loads, structures are often subjected to stress levels that go well beyond the material's elastic limit, causing residual damage and nonlinear deformations. To capture this behavior and obtain reliable results, computational models in the form of nonlinear finite element models combined with state-of-the-art material model formulations are employed for the structural system and materials of the building alternative investigated (e.g., reinforced concrete moment frames, wood shear wall systems, etc.).

The choice of the finite element model type for a given application requires a fine balance between accuracy, practicality, and computational efficiency, subject to the capabilities of available software and computational resources [79]. For the most accurate results, it is recommended that the building alternatives be modeled and analyzed using 3D approaches. However, depending on the combination of natural hazard and structural system being considered, the main load-resisting mechanisms of the building may allow for the use of modeling strategies that reduces computational costs with low accuracy compromises. In addition to the building alternatives considered, if the building-foundation interaction is of interest and/or is expected to significantly influence the building's response – such as during earthquake events – their foundation may also be included in the model. The boundary conditions are defined as realistically as possible for all the elements of the building, including the foundation and soil, if considered. Examples of different modeling strategies are discussed in detail in the case study sections of this study (see Section 3.1).

2.2. Structural assessment to natural hazard loads

Adequate characterization of the natural hazard load on the structure is essential to calculate accurate building performance and damage. Natural hazard loads are usually dynamic (i.e., time-dependent) in nature as they normally develop over a short period of time (e.g., windstorm, earthquake, tsunami, etc.). Nonlinear time-history analysis is broadly adopted in PBD and is considered the most realistic approach to model natural hazard loads as it imposes time-dependent load behaviors such as rate-dependent effects and path-dependent cyclic loads [79] on the computational building models. This type of analysis, however, is computationally demanding and can take significant time to complete depending on the natural hazard, computational building model, and computational resources. Alternatively, nonlinear static analysis – where the time-dependent effects are not considered – is a much simpler computational procedure that, despite its lower accuracy, can be used when there are limited computational resources and sufficient literature evidence that demonstrate its applicability and limitations to nonlinear time-history analyses [14,80].

The determination of the full response of the building alternatives from their initial elastic to the near-collapse-nonlinear stages is required for the characterization of the expected damage levels on each performance limit state considered (discussed in Section 2.3). To calculate the full building response, each computational model is subjected to a series of discrete natural hazard loads that range from reasonably low-intensity values (e.g., 0.5 m tsunami inundation depth, 0.05 g earthquake peak ground acceleration, etc.) to the intensity that initiates the building collapse.

2.3. Performance limit states determination

The determination of performance limit states defines thresholds for the expected damage levels of the building alternatives under natural hazard loads and is an essential step of the PBD methodology. In the proposed framework, these limit states are the foundation for the calculation of the performance-based life-cycle assessment (Section 2.4) and the performance normalization indexes (Section 2.5). Despite being subjective to the specific desires of the decision-makers, a set of four limit states are used in the proposed framework to characterize the building's performances as recommended in modern PBD guidelines [3,81]: operational (OP), immediate occupancy (IO), life safety (LS), and collapse prevention (CP). As shown in Fig. 2, the OP indicates the state at which the structure has suffered no damage and requires no evacuation during the natural hazard; the IO indicates the state at which the structure retains its pre-natural hazard strength and stiffness, and can be re-occupied immediately; the LS indicates the state at which the structure has some damaged components but is safe against the onset of a partial or total collapse; and the CP indicates the state at which the structure has suffered major damage, without complete collapse, and requires a complete demolition [81].

These performance limit states are defined based on engineering demand parameters (EDP) that best represent the effects of the natural hazard loads on the building (e.g., interstory drift ratios, deformations, individual element rotations, etc.). To define the EDPs corresponding to each performance limit state, this study employs a simplified discrete approach where the computational model of each building is subjected to fictional loads that aim at primarily engaging their main load-resisting mechanism for the natural hazard considered. This approach is similar to analysis procedures available in first-generation PBD manuals [82]. To allow capturing the post-peak responses of each building alternative, the fictitious loads are applied in a displacement-controlled manner. If the main load-resisting mechanism of the building alterna-

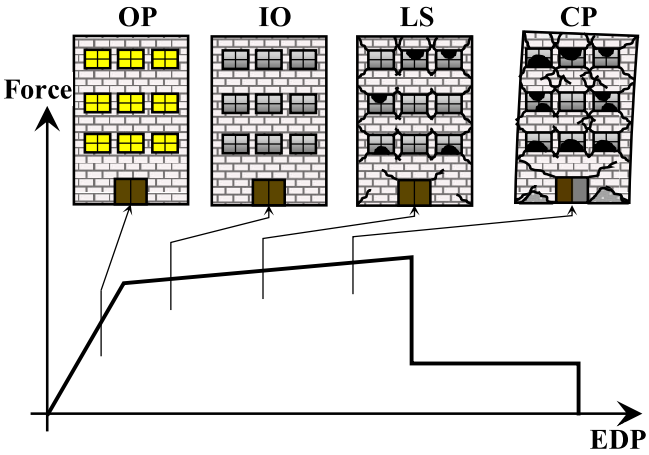

Fig. 2. Performance limit states based on structural load-deflection response.

tive investigated involves complex structural interactions that are not easily representable by displacement-type fictitious loads, the results calculated in the structural assessment stage can be used to define the performance limit states. The case study section of this study provides an example of EDP determination (see Section 3.4).

2.4. Process A: performance-based life cycle assessment (LCA)

The LCA analysis is used to evaluate the environmental impacts of each building alternative over its entire lifespan. In addition to the usual cradle-to-grave LCA analysis of buildings, the calculated natural-hazard structural performance of each building has a direct impact on the calculated results, as shown in Fig. 3. If no natural hazard occurs, the building operates normally until the end of its lifespan, when it is demolished, and its materials are sent to recycling. In the event of a natural hazard, the building's structural performance determines the endured damage level (which may include building collapse), and the appropriate post-disaster retrofit measures are performed. Finally, the LCA results at each building limit state's damage threshold are used to calculate performance-based environmental impact results (i.e., environmental impacts per limit state).

The cradle-to-grave LCA analysis is based on the ISO 14040 [45] and ISO 14044 [46] guidelines and the functional unit is defined based on key common properties of the different building alternatives considered (e.g., total floor area, number of stories, performance criteria used during design, etc.). In practice, the functional unit should represent a common goal sought by all the investigated building design alternatives. This definition is essential so that the environmental impacts of each building alternative can be guaranteed to be the result of the pursuit of a common goal, which is essential for their effective comparison.

The proposed framework subdivides the environmental impacts into six distinct phases: material manufacturing, building construction, use, retrofit, demolition, and material recycling, as shown bolded in Fig. 3. The material manufacturing and construction phases group the main operations required to erect the original and retrofitted (or reconstructed, in case of collapse) building, including the shipping of the essential materials. The use phase of a building groups the impacts associated with heating and cooling, electricity use, water use, etc. and can be omitted in the analysis (dashed line in Fig. 3) if sufficient literature evidence demonstrates similar environmental impacts during this phase for the different building alternatives considered. In addition, the impacts of the use phase are usually not significant when the damage and retrofit impacts are assessed in separate phases [83], as in the proposed framework. The retrofit phase groups the post-natural hazard-induced operations required to restore any non-collapsible damage. The demolition phase groups the operations performed to demolish or disassemble the building at the end of its lifespan or to account for post-disaster operations performed on collapsed structures (e.g., the demolition of any remaining sections, gathering of debris, site cleaning, etc.). Finally, the recycling phase is conducted when the building is either demolished at the end of its lifespan or when it collapses. In the latter case, a reduced recycling ratio is considered to reflect material losses that might occur due to the collapse of the building (e.g., damage beyond repair, material carried away by the waves/wind, etc.).

For each phase, the environmental impact is evaluated in terms of the inflow (material and energy consumption) and resultant outflow (waste generation and emissions) that influences the ecosystem and human health [71,84]. The inflows are calculated in the life cycle inventory analysis, where all the activities in each LCA phase are identified and their required amounts of raw material and energy are listed. Finally, the collected inventory data is evaluated using an impact assessment method (e.g., TRACI 2.1) which translates the LCI input data into "meaningful" environmental impacts for different categories. The proposed framework includes six impact categories, following the recommendation of FEMA P-58 [83] for the environmental assessment of buildings subjected to natural hazard loads: global warming potential (GWP) including and excluding CO_2 sequestration by wood products, acidification (AC) potential, eutrophication (ET) potential, ozone depletion in the air (ODA), and smog air (SA) potential.

2.5. Process B: performance normalization index

Different building alternatives designed to resist the same natural hazard load can have significantly different structural performances if they were to be physically tested or numerically analyzed using nonlinear computational models. This occurs because applicable building codes provide only the minimum design requirements that result in a hard-to-quantify performance. The main argument of the proposed framework is that the structural performance of the building alternatives investigated should be equivalent in order to enable a direct quantitative comparison of their environmental impacts. While one solution to this problem would be to iteratively adjust the building designs until the computational models indicate identical structural performances, this approach is not feasible due to the high computational and time demand required by nonlinear numerical analyses. To overcome this limitation, this study proposes the calculation of Performance Normalization Indexes (PNI), which is a considerably simpler approach that normalizes the performance limit states of each building alternative (Equa-

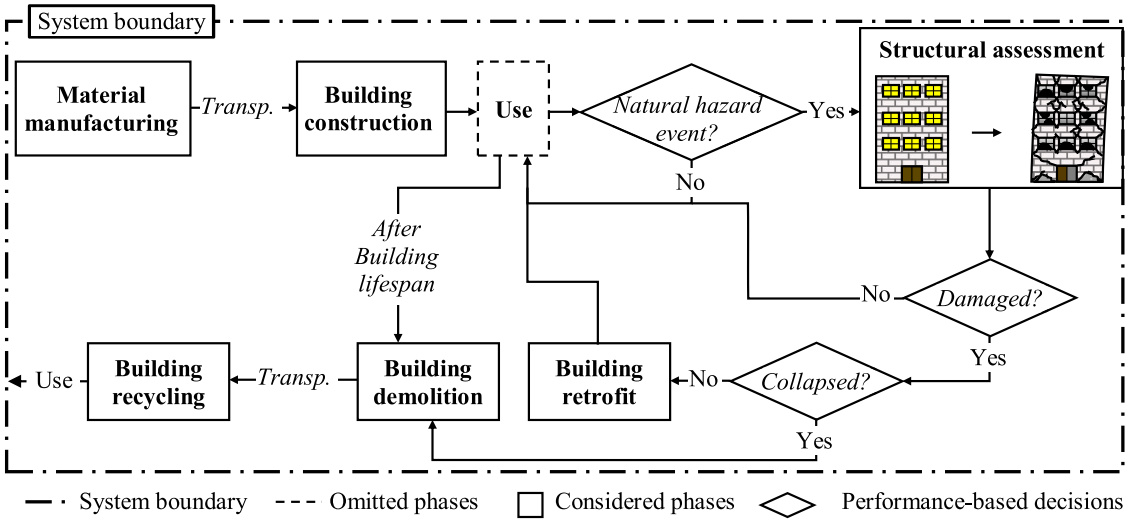

Fig. 3. System boundary and LCA phases considered.

tion (1)). As shown in Fig. 4, the PNI represents the magnitude of the difference in calculated force and EDPs between two building alternatives. Equation (1) also includes weighting factors that allow decision-makers to express which equation term (EDP or force) to prioritize depending on their desired building performance. For instance, the difference in the calculated EDP may be prioritized (i.e., it has a higher "weight" in the decision process) rather than the difference in sustained force magnitude. If the EDP is to have double the "importance" of the force magnitude, this priority can be expressed in the PNI calculation by setting the EDP weighting factor to 2. To calculate the PNI, one of the investigated building alternatives is treated as the reference building (e.g., building 2 in Fig. 4) for which the calculation of the PNI is not required. For all other building alternatives considered (two are considered in Fig. 4, but more could be added), Equation (1) is used for each limit state considered.

$$PNI_{ji} = \sqrt{\frac{\delta_{edp}}{\delta_f}\left(\frac{edp_{bj_i}}{edp_{bref_i}}\right)^2 + \frac{\delta_f}{\delta_{edp}}\left(\frac{F_{bj_i}}{F_{bref_i}}\right)^2} \quad (1)$$

where PNI_{ji} is the performance normalization index of building j at performance limit state i, b_j is building j, b_{ref} is the reference building, the F_{bji} is the force for building j at limit state i, δ_{edp} is the EDP weighting factor (≥1), and δ_f is the force weighting factor (≥1). Fig. 4 shows the visual representation of the PNI where i equals CP, j equals building 1, and *ref* equals building 2.

2.6. Normalized performance-based environmental assessment

In the last step of the proposed framework, the calculated PNIs and environmental impacts are used to obtain the "normalized structural performance-based environmental impacts" of each investigated building design alternative. This is achieved by dividing the performance-based environmental impacts calculated in Process A by the PNIs calculated in Process B, as expressed by Equation (2). This normalized impact is calculated only for the non-reference buildings, as defined in Process B, and modifies their environmental impacts to account for the difference in structural performance. By normalizing to an equivalent structural performance, a building design alternative can have its calculated environmental impacts artificially modified (i.e., reduced or augmented) based on the difference in structural performance to the reference building. For instance, if two design alternatives with similar environmental impacts are being considered, the normalized structural performance-based environmental impacts of the design alternative with better structural performance would be reduced.

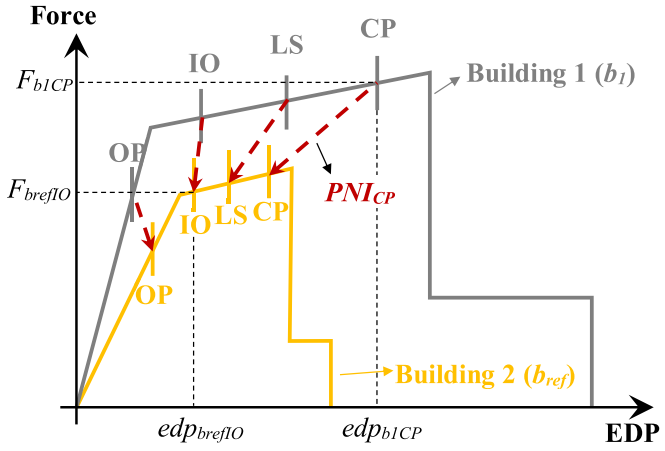

Fig. 4. Performance comparison and normalization factors.

$$E_{pbji} = \frac{E_{ji}}{\delta_{sp} PNI_{ji}} \quad (2)$$

where E_{pbj} is the performance-based environmental impact of building j at limit state i, E_{ji} is the environmental impact of building j at limit state i, $PNIji$ is the performance normalization index of building j at limit state i, and δ_{sp} is the structural performance weighting factor (>0).

Similar to the calculation of the PNIs in Equation (1), Equation (2) also includes a weighting factor that provides flexibility to decision-makers to express which equation term (i.e., environmental impact or structural performance) to prioritize. For instance, if structural performance has twice the "importance" of environmental impact for a given situation, the structural performance weighting factor can be set to 2 and the normalized environmental impacts will be doubly affected by the structural performance difference expressed by the PNIs.

3. Case study: cross laminated timber and reinforced concrete

For demonstration purposes, the proposed framework is employed to investigate and compare the tsunami structural performance-based environmental impacts of a seven-story building made of two different structural materials: cross laminated timber (CLT), which is a relatively new and eco-friendly material, and traditional reinforced concrete (RC) materials. While this case study focuses on the structural performance to tsunami loads, which is a relatively unexplored research area, the framework could also be applied to other natural hazard loads such as seismic or windstorm loads.

The CLT building has been constructed as part of a previous study by others to evaluate the earthquake performance of multi-story CLT buildings [85], as shown in Fig. 5. It was originally designed following Eurocode 8 [86] guidelines to resist the peak ground accelerations of the Kobe JMA earthquake, one of the most devastating earthquakes of the past decades. Spruce CLT panels are used for the walls, floors, and roof slabs. Due to different structural needs, several CLT wall thicknesses are used on different stories. Self-drilling screws are used to connect floor slabs to CLT walls and adjacent wall/slab panels. In addition, angle brackets and hold-downs are used to connect the wall panels to the slabs and the foundation (see Fig. 5a for the distribution of the connections on the first floor of the building). More details on the CLT building design can be found at [85].

The RC building was designed specifically for this study following the same guidelines and load intensities used for the CLT building in order to ensure an "equivalent structure", as shown in Fig. 5. The design characteristics of each story of the RC moment frame building are shown in Table 1. Masonry infill walls are used to provide enclosure to the outer shell of the building while the interior walls are made of non-structural elements such as drywall or light steel framing.

3.1. Computational models of the building alternatives

As discussed in Section 2.1, the main load-resisting mechanisms of the RC and CLT buildings allowed for the use of different modeling strategies to reduce computational costs with minimum accuracy compromises. For the moment frame RC building alternative, lateral loads caused by the tsunami are mainly resisted by the frames in the direction of the load. In regular moment frame buildings (i.e., box-shaped with no stepped elevations) such as the one considered in this study, it is common to analyze only one of the building's bays and reasonably assume the same response for the remaining identical bays (e.g., Refs. [19,87]). Thus, for this combination of natural hazard and building alternative, a 2D modeling approach was used. On the other hand, in panelized building alternatives such as CLT building, the three-dimensional interactions between in- and out-of-plane wall panels are the main load-resisting mechanism. Consequently, a 3D modeling approach was used.

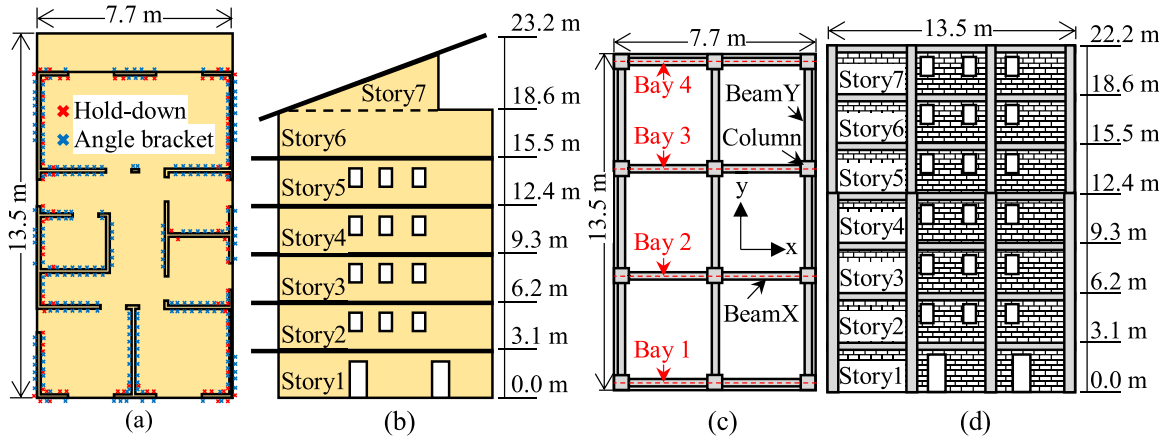

Fig. 5. –Plan and elevation views of the seven-story (a)–(b) CLT [85] and (c)–(d) RC buildings.

Table 1
Design details of the RC building.

Story	Column			Beams			
				Dimens. (m x m)	Long. Reinf.		Transv. Reinf.
	Dimens. (m x m)	Long. Reinf	Transv. Reinf.		BeamX	BeamY	
1	0.6 x 0.6	12-#11	3-#4@125 mm	0.4 x 0.3	6-#10	6-#11	2-#4@220 mm
2	0.6 x 0.6	8-#10	2-#4@125 mm	0.4 x 0.3	6-#10	6-#11	2-#4@220 mm
3	0.6 x 0.6	8-#10	2-#4@125 mm	0.4 x 0.3	6-#10	6-#11	2-#4@220 mm
4	0.6 x 0.6	8-#10	2-#4@125 mm	0.4 x 0.3	6-#10	6-#11	2-#4@220 mm
5	0.5 x 0.5	8-#10	2-#4@180 mm	0.4 x 0.3	4-#10	4-#11	2-#4@300 mm
6	0.5 x 0.5	8-#10	2-#4@180 mm	0.4 x 0.3	4-#10	4-#11	2-#4@300 mm
7	0.5 x 0.5	8-#10	2-#4@180 mm	0.4 x 0.3	4-#10	4-#11	2-#4@300 mm

The finite element details of each developed model are discussed in Appendix A.

3.2. Structural assessment to tsunami loads

Characterization of the tsunami load was performed using a triangular static-equivalent lateral hydrodynamic force, which is the approach proposed in current design guidelines [88] that has been shown to provide good predictions of structural responses when compared to a wide range of dynamic time-history analyses [87]. The force per building's unit width is calculated based on the tsunami flow regime (i.e., subcritical or choked). To allow the use of the new tsunami chapter of ASCE 7 [88] to perform the tsunami analysis (which is based on mapped inundation depths of the United States), the structures are considered to be located in Blaine, Washington. At the building location, the inundation depth and flow velocity are calculated to be 2.4 m and 4.5 m/s, respectively, using the energy grade line analysis method of ASCE 7 [88], which results in a Froude number of 0.93. As indicated in Ref. [87], the critical Froude number for a building located in a sparse environment is 0.68; consequently, the tsunami flow considered in this study is in the choked regime, and the force per unit structural width was calculated using Equation (3) [89].

$$\frac{F}{b} = \lambda \rho g^{1/3} u^{4/3} h^{4/3}, \ if \ F_r \geq F_{r,c} \tag{3}$$

where F is the tsunami force, b is the width of the building, ρ is the density of the fluid, u is the flow velocity, h is the inundation depth, g is the acceleration of gravity, F_r is the Froude number ($u/\sqrt{gh}$), and λ is the leading coefficient [89].

In the 3D CLT computational building model, the tsunami force was applied as a triangular pressure distribution from the bottom of the building to the inundation depth considered, as shown in Fig. 6. In the

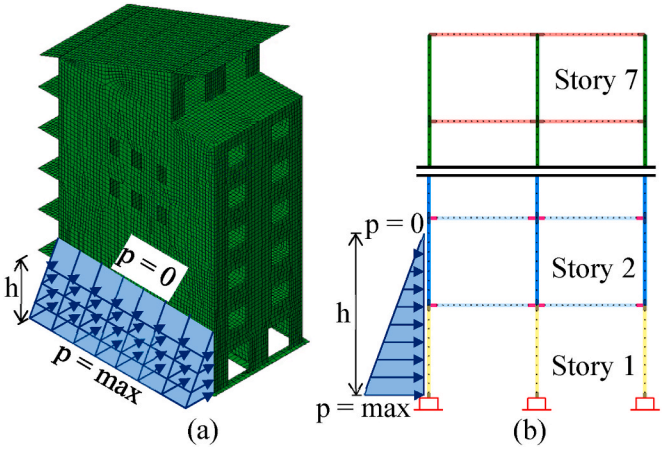

Fig. 6. Tsunami load application approach on (a) CLT and (b) RC models.

RC model, a tributary distance was used to convert the water pressure into an equivalent triangular force. The tributary distance was considered before and after the masonry infill walls collapsed due to the tsunami. Before the infill walls collapsed, they were assumed to effectively transfer the loads to the adjacent moment frames and the tributary distance was taken as the distance between the moment frames of the building. After the infill walls collapsed, they were assumed to be carried away by the wave, making the load affect only the moment frame itself. In this case, a reduced tributary distance equal to the width of the RC columns was considered. The maximum out-of-plane load that the infill walls can resist was calculated using [90].

In this study, the wave was considered to afflict the longest side of the buildings, as shown in Fig. 6, as this side provides the largest area for the development of the tsunami pressure. The two building alterna-

tives were subjected to a series of tsunami inundation depths starting at 0.5 m and increasing by 0.5 m until their collapse. The flow velocity at each inundation depth was calculated assuming a constant Froude number, which is considered a realistic assumption as shown in typical tsunami onshore flow time histories [87].

3.2.1. Calculated buildings' response to tsunami-load

No significant damage was calculated for the CLT building under inundation depths below 3.0 m (i.e., approximately the height of the first story). As inundation depths increased, an increasing number of CLT panel connections on the first story of the side afflicted by the tsunami load failed. With a reduced number of panel connections (after failures), increased loads were re-distributed to adjacent connections until the maximum resisted inundation depth of 6.0 m (i.e., approximately the height of the second story). For larger inundation depths (i.e., 6.5 m), all of the first story panel connections on the side afflicted by the tsunami load failed, which significantly increased the stresses and caused the failure of the long-span CLT wall panels, as shown in Fig. 7a. The stresses on the short-span walls were not enough to cause their failure due to the restraint provided by the in-plane walls, which contributed to reducing the span and, consequently, the tsunami-applied bending moments. Despite the survival of the shorter walls, it was assumed in this study that the failure of the long-span walls would cause tsunami loads to penetrate the building and fail the interior walls. Since CLT wall panels comprise the main structural system of the building, this inundation depth was considered to initiate the building collapse.

For the RC building, no significant damage was calculated until the tsunami inundation depth reached 2.0 m, where minor cracks occurred at the bottom of the first story columns. As inundation depths increased, the cracks widened and propagated along the beams and columns of the first stories. At an inundation depth of 5.0 m, the first reinforcing steel yielding occurred at the base of the first story columns. At the maximum resisted tsunami inundation depth (i.e., 8.0 m), extensive cracking was calculated in the first three stories of the building and several reinforcing steels experienced post-yield stress levels, with many approaching the rupture stress, as shown in Fig. 7b. For larger inundation depths investigated (i.e., 8.5 m), the building collapsed due to reinforcing steel rupture and extensive damage to the first story beams and columns.

3.3. Performance limit states determination

The first story interstory drift (ISD) ratio was selected as the EDP to define the performance limit states of the two building alternatives. ISD is the most common EDP for the PBD analysis of buildings and has been extensively used to investigate the performance under earthquake loads. Since tsunamis also impose lateral loads, several studies have used the ISD as EDPs for tsunami performance assessment (e.g., Refs. [87,91]). Two approaches were used to determine the performance limit states for the CLT and RC buildings due to the fundamental differences in their main tsunami load-resisting mechanisms (discussed in Section 3.1). For the RC building, displacement loads were increasingly applied at the first story level of the building. This approach is used because it represents the main tsunami load-resisting mechanism of RC buildings, which is the first story moment frame lateral resistance (as indicated by the results of the computational building models discussed in Section 3.2). Since the main tsunami load-resisting mechanism of the CLT building involved the interaction between the in- and out-of-plane panels, a fictitious displacement-type load could not be easily derived. Thus, the calculated response to the highest imposed tsunami inundation depth was used. The two buildings responses are shown in Fig. 8.

For the RC building, the ISD ratios corresponding to each performance limit state are defined following the recommendations of ASCE 41 [81] as the drift at which: the first cracking occurred for the OP limit state, minor cracking and limited yielding occurred at a few locations for the IO limit state; extensive damage to beams, shear cracking in ductile columns, and joint cracks occurred for the LS limit state, and extensive cracking in ductile elements and severe damage in columns for the CP limit state. For the CLT building, the ISD ratios are defined as the drift at which: the first connection failed for the OP and IO limit states, all of the connections of a single wall panel failed for the LS limit state, and as 75% of the collapse drift for the CP limit state. The ISD values are summarized in Table 2.

Fig. 9 compares the first story ISD versus the inundation depths calculated in Section 3.2 for each building alternative. Similar ISDs were calculated until an inundation depth of 5.5 m. At higher inundation depths, the softer response caused by the damaged beams and columns caused the RC building's ISD to increase significantly. At their respective maximum resisted inundation depths, the first-story drift of the RC building was approximately 4.8 times higher than that of the CLT building, as shown in Fig. 9, which indicates that the ductility (an indicator of the energy absorbed by the building) of the CLT building was

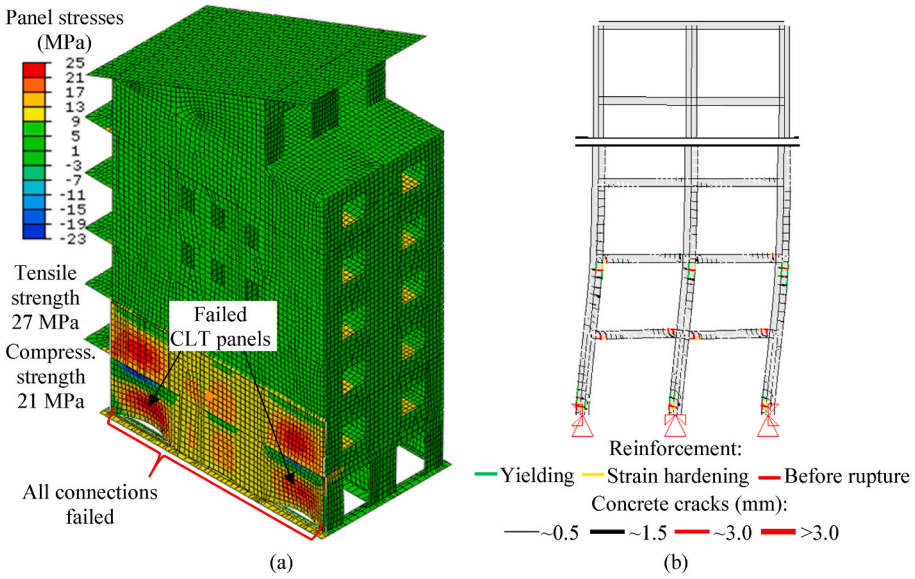

Fig. 7. (a) CLT and (b) RC building response at the highest resisted tsunami inundation depth.

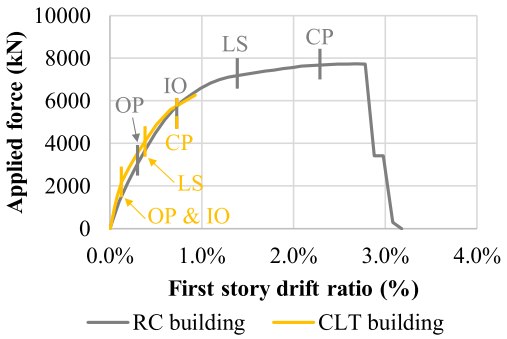

Fig. 8. CLT and RC building response to determining performance limit states.

Table 2
Performance limit states for the CLT and RC buildings.

Performance Limit	Force (kN)		ISD	
	CLT Building	RC Building	CLT Building	RC Building
Operational (OP)	2198	3024	0.13%	0.30%
Immediate Occupancy (IO)	2198	5599	0.13%	0.70%
Life Safety (LS)	4229	7184	0.40%	1.40%
Collapse Prevention (CP)	5583	7688	0.66%	2.30%

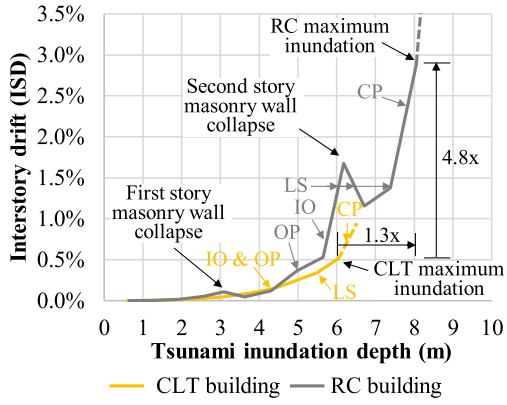

Fig. 9. First story drift versus inundation depth response.

approximately 80% lower than that of the RC building. The maximum resisted inundation depth of the RC building was 1.3 times higher than that of the CLT building. In addition, the overall structural performance of the CLT building was considerably lower than that of the RC building as indicated, for example, at the tsunami inundation depth of 5.8 m, where the CLT building experienced post-LS responses while the RC building was at the IO performance limit state.

3.4. Process A: performance-based life cycle assessment analysis

The functional unit for the LCA analysis was defined as a 13.5 m x 7.7 m seven-story building designed according to Eurocode 8 [86] to resist the peak ground accelerations of the Kobe JMA earthquake, which are common properties of the CLT and RC buildings considered. The life cycle inventory (LCI) data were site-specific, based on recent technologies and normal production conditions. The main assumptions made to compile the LCI inputs and quantify the outputs of each LCA phase (including the retrofit approaches considered) are discussed in detail in Appendix B. The environmental impacts were calculated based on the LCI inputs using TRACI 2.1 [92] characterization factors and the LCA software GaBi [93]. The use phase was not included in the framework as previous studies have demonstrated similar environmental impacts for CLT and RC buildings (e.g., Ref. [94]).

3.4.1. Reference environmental impact results

Reference environmental impacts (i.e., where no tsunami damage occurs) are shown in Fig. 10. For each category, the 100% impact is attributed to whichever building alternative with the highest environmental impact for that category. The large amounts of energy required to produce RC resulted in 81% of the total impacts of the RC building being attributed to its material manufacturing phase. For some of the impact categories, this phase alone resulted in environmental impacts higher than the total impacts of the CLT building. For the CLT building, the total environmental impacts were better distributed throughout the different LCA phases with the construction phase resulting in the largest contribution of, on average, 36% of the total environmental impacts. The total environmental impacts of the CLT building were, as an average of all investigated impact categories, 39% lower than those of the RC building. This result agrees with the findings of previous studies (e.g., Refs. [95–97]) and validates the life cycle data calculated in this study. Different from the other impact categories, the ODA and SA impacts of the CLT building were significantly higher and comparable to those of the RC building. This result occurred due to the large shipping distance (i.e., 777 km) from the CLT manufacturing plant to the building site. This is one of the existing limitations of constructing with CLT materials as only a few manufacturers are currently available in North America (i.e., about 10) compared to much more prevalent concrete plants. The detrimental environmental effects of large CLT travel distances have also been confirmed by previous literature studies (e.g., Ref. [98]). In this study, a "favorable" scenario in terms of shipping distances occurs as most of the CLT plants in North America are located on the west coast. Consequently, projects in different areas would likely require longer travel distances.

3.4.2. Tsunami-induced environmental impact results

Fig. 11 shows the environmental impacts associated with the tsunami-induced damage of the CLT and RC buildings calculated in Section 3.2. The impacts at the inundation depth of zero meter are equivalent to the reference impacts shown in Fig. 10, i.e., the reference impacts. It is shown that the increase in total environmental impacts caused by the retrofit actions on the CLT building was insignificant when compared to its reference impacts (see the damage and undamaged results in Fig. 11). A similar result was observed for the RC building until the point where RC jacketing was required. After

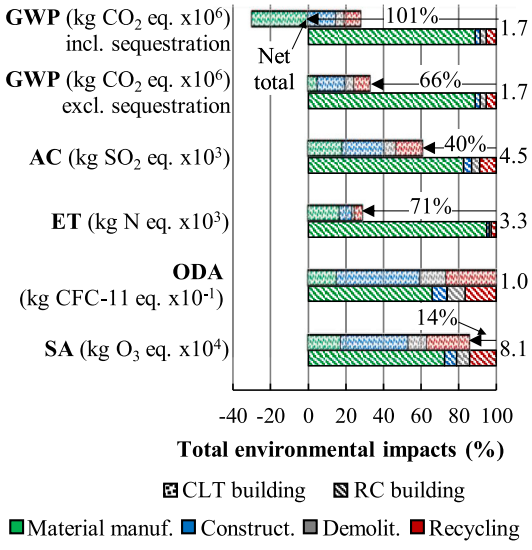

Fig. 10. Life cycle assessment results for CLT and RC buildings.

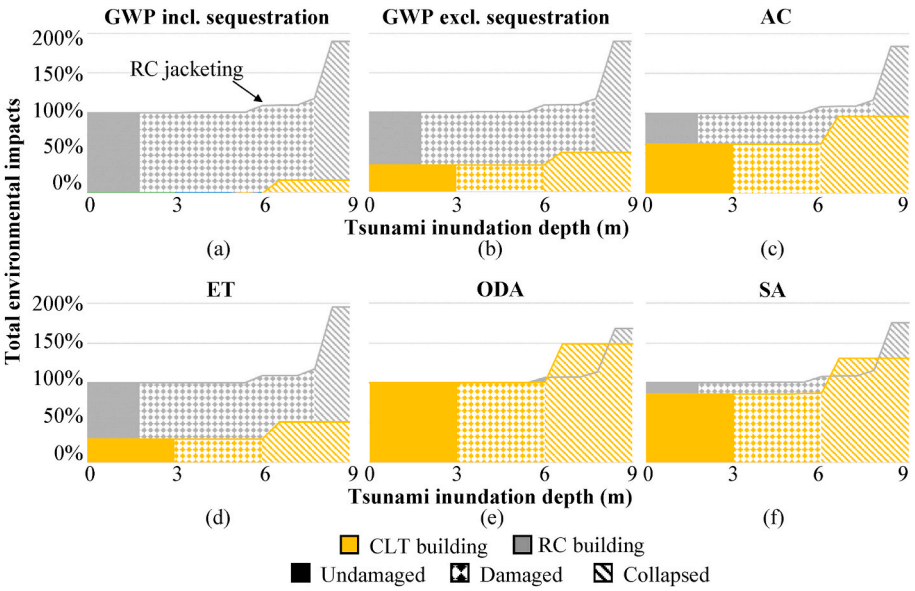

Fig. 11. Life cycle assessment for the CLT and RC buildings under different tsunami inundation depths.

this inundation depth, a noticeable increase in the environmental impacts of the RC building (i.e., ~9%) in all impact categories was observed, as indicated in Fig. 11a. The most significant environmental impact increase for the two building alternatives occurred when the buildings collapsed due to the tsunami, causing a 30% and 82% increase, on average for the CLT and RC buildings, respectively. The larger environmental impact increase of the RC building is attributed to the significant environmental impacts of its material manufacturing phase, as discussed in Section 3.4.1.

For most of the impact categories analyzed, the environmental impacts of the CLT building were sufficiently lower than that of the RC building to the point that not even its collapse (at 6.5 m) resulted in environmental impacts above those of the RC building, as shown in Fig. 11a–d. The ODA and SA were the only categories in which this result was not applicable since, at inundation depths between the collapse of the CLT and RC buildings (i.e., between 6.5 m and 8.5 m), the CLT building resulted in higher environmental impacts than the RC building, as shown in Fig. 11e and f.

The environmental impacts per tsunami inundation depth shown in Fig. 11 can be categorized by limit state using the values calculated in Section 3.3, as shown in Fig. 12. As higher tsunami inundation depths subject the building structures to increased damage and, consequently, higher limit states, Fig. 12 displays the same relationship between the RC and CLT buildings discussed in Fig. 11.

3.8. Process B: performance normalization index

Based on the defined ISDs and the corresponding force levels for each performance limit state (see Fig. 8), Equation (1) was used to calculate the Performance Normalization Indexes (PNI) for the RC building while the CLT building was treated as the reference building. No priority was given to force over EDP (i.e., the force and EDP weighting factors were set as 1). The PNI results are summarized in Table 3.

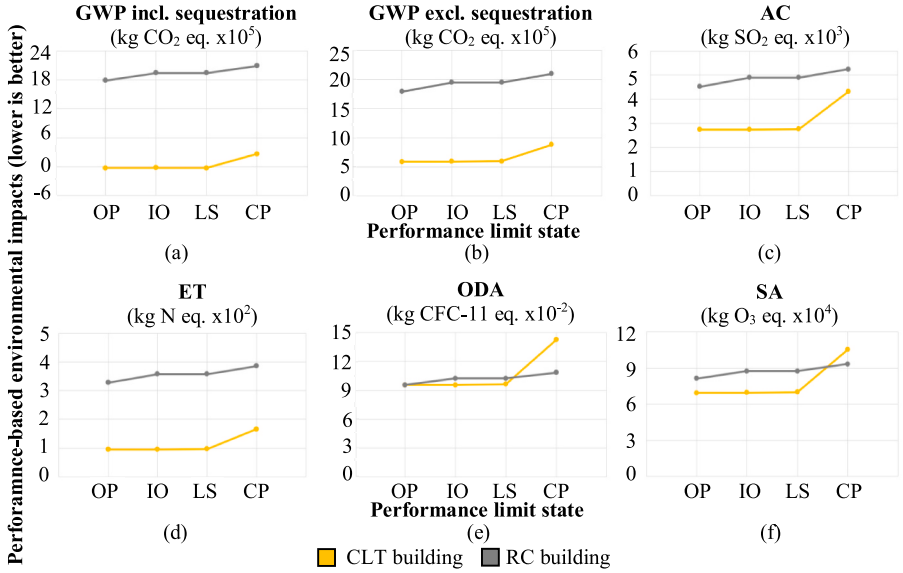

Fig. 12. Performance-based – Performance-based environmental impacts of the investigated buildings.

Table 3
Performance normalization indexes for the RC building.

Performance Limit	Performance Normalization Indexes (PNI)
Operational (OP)	2.7
Immediate Occupancy (IO)	6.0
Life Safety (LS)	3.9
Collapse Prevention (CP)	3.7

3.6. Normalized performance-based environmental assessment

The PNIs were used to calculate the structural performance-based environmental impacts of the RC building to allow the effective quantitative comparison of the environmental impacts and structural performance of the CLT and RC buildings. In calculating the normalized environmental impacts for each performance limit state, no priority was given to structural performance over environmental impacts (i.e., the structural performance weighting factor was set as 1). The results are shown in Fig. 13. A direct comparison between the results in Figs. 13 and 12 (repeated in dashed lines in Fig. 13) clearly shows the effect of the use of the PNIs to obtain the performance-based environmental impact. When the calculated environmental impact results were not normalized using the PNIs, the CLT building resulted in lower impacts than the RC building in nearly all of the impact categories investigated. In Fig. 13, where the PNIs have been used to account for the difference in the structural performance of each building alternative, the RC building resulted in lower performance-based environmental impacts than the CLT building for nearly all of the impact categories.

The performance-based environmental impact results in Fig. 13 also allow in-depth analyses of the two building alternatives considered. Firstly, for the OP limit state of the GWP (excluding sequestration) and the ET categories, the CLT building resulted in lower performance-based environmental impacts. This occurred because, at the first performance limit state, the structural performance of the two building alternatives were similar, as discussed in Section 3.3 and shown in Fig. 9. In this case, the difference in structural performance did not play a major role in the assessment while the difference in sustainability governed the determination of the favorable building alternative. Secondly, in the AC, ODA, and SA impact categories, the RC building resulted in lower normalized environmental impacts for all performance limit states investigated. This occurred because these impact categories were the ones with the lowest difference in environmental impacts between the CLT and RC buildings, as shown in Fig. 11. Consequently, when the significantly different structural performances of the two building alternatives were normalized using the PNIs, the RC building resulted in the most favorable alternative. Lastly, in the GWP (including sequestration) category, the CLT building resulted in lower normalized environmental impacts for all performance limit states considered. This result is directly related to the majority of the CLT structural system being comprised of wooden panels, which act as a carbon sink (i.e., provided that it comes from sustainably managed forests). This allows the CLT building to significantly diminish its carbon footprint, especially in comparison to traditional material alternatives such as reinforced concrete.

4. Summary and conclusions

This study presented the first attempt at a multidisciplinary framework that combines performance-based design and life cycle assessment to enable the effective comparison of the structural performance-based environmental impacts of different building alternatives. The framework relies on the accurate characterization of the building's performances by means of state-of-the-art computational models subjected to discrete, static-equivalent natural hazard loads. This characterization is used to define response thresholds of four limit states: operational, immediate occupancy, life safety, and collapse prevention. The buildings responses at each limit state are used for two concurrent objectives: to calculate a performance-based cradle-to-grave life cycle assessment that accounts for natural-hazard induced damage; and to calculate a performance normalization index (PNI), which quantifies the magnitude of the difference in structural performance to natural hazards between the investigated buildings. Finally, the calculated environmental impacts are modified by the PNIs to reflect the investigated buildings' differences in structural performance.

The contribution of the developed framework in revealing the trade-offs among different design alternatives and effectively supporting decision-making processes is demonstrated in the comparison of two seven-story buildings in a tsunami-prone region: a cross laminated timber (CLT) building and a reinforced concrete (RC) building. The RC building was shown to have better structural performance to tsunami loads while the CLT building had lower environmental impacts. The use of the proposed framework through the calculated PNIs indicated that, when the difference in structural performance between the two building alternatives was considered, the RC building presented lower normalized environmental impacts than the CLT building for the majority

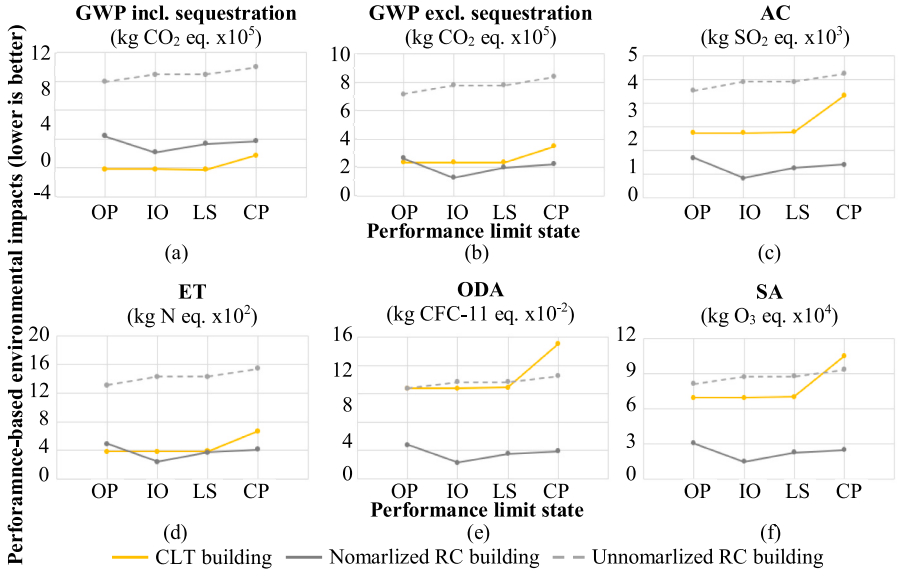

Fig. 13. Normalized performance-based environmental impacts.

of environmental impact categories and performance limit states investigated. Thus, the use of the proposed framework indicated that lower structural performance to natural hazard loads can offset the benefits of a building alternative with lower environmental impacts. The magnitude of the offset depends on the combination of the building alternatives, performance limit states, and environmental impact categories are considered.

In order to make the first iteration of the proposed framework as simple and practical as possible, there are limitations to the current study. First, a discrete hazard analysis approach was considered in the development of the framework, which reflected the first-generation PBD procedures. Current-generation PBD approaches already include stochastic and probabilistic methods that produce statistical outcomes that account for risk levels associated with the probability of different natural hazard recurrence intervals on random building alternatives, locations, and natural hazard load conditions. Second, the framework considers isolated natural hazards only, while the performance-based study of multi-hazard events has been significantly developed in recent years. Third, simplified static-equivalent analyses are used in the framework to obtain building performances, which lack accuracy on building alternatives with plan and elevation irregularities, or where the contributions of higher mode effects are expected to be significant. Fourth, the framework's life-cycle assessment includes only environmental impact determination of the structural members of the building. The life-cycle assessment can be expanded to include non-structural members and other non-environmental aspects such as economic impacts, societal impacts, effects of damaged building's downtime, different energy matrices, etc.

CRediT authorship contribution statement

Rafael A. Salgado: Conceptualization, Methodology, Validation, Formal analysis, Investigation, Data curation, Writing – original draft, Visualization. **Serhan Guner:** Conceptualization, Methodology, Resources, Writing – review & editing, Supervision, Funding acquisition.

Declaration of competing interest

The authors declare that they have no known competing financial interests or personal relationships that could have appeared to influence the work reported in this paper.

Acknowledgments

The authors would like to thank Dr. Defne Apul for the advice and resources used to perform the life cycle impact assessment in this study.

Appendix A. Supplementary data

Supplementary data to this article can be found online at https://doi.org/10.1016/j.jobe.2021.102908.

References

[1] U.S. Indian Ocean Tsunami Warning System Program, How resilient is your coastal community? - a guide for evaluating coastal community resilience to tsunamis and other hazards, 2007. https://www.fema.gov/media-library/assets/documents/90380.

[2] C. Menna, D. Asprone, F. Jalayer, A. Prota, G. Manfredi, Assessment of ecological sustainability of a building subjected to potential seismic events during its lifetime, Int. J. Life Cycle Assess. 18 (2013) 504–515, https://doi.org/10.1007/s11367-012-0477-9.

[3] Federal Emergency Management Agency (FEMA), Seismic performance assessment of buildings, Methodology, FEMA P-58-1 Publication, 1, 2012, p. 278.

[4] FEMA, Guidelines for performance-based seismic design of buildings, Fema (2018) 92 P-58-6. 6 https://www.fema.gov/media-library/assets/documents/90380.

[5] H. Ghaffarzadeh, N. Talebian, R. Kohandel, Seismic demand evaluation of medium ductility RC moment frames using nonlinear procedures, Earthq. Eng. Eng. Vib. 12 (2013) 399–409, https://doi.org/10.1007/s11803-013-0181-1.

[6] S.C. Goel, W.-C. Liao, M. Reza Bayat, S.-H. Chao, Performance-based plastic design (PBPD) method for earthquake-resistant structures: an overview, Struct. Des. Tall Special Build. 19 (2009) 115–137, https://doi.org/10.1002/tal.547.

[7] F.K.H. Zareian, Simplified Performance Based Earthquake Engineering, 2009 Stanford, CA.

[8] R.A. Salgado, S. Guner, A comparative study on nonlinear models for performance-based earthquake engineering, Eng. Struct. 172 (2018) 382–391, https://doi.org/10.1016/j.engstruct.2018.06.034.

[9] A.A. Hedayat, H. Yalciner, Assessment of an existing RC building before and after strengthening using nonlinear static procedure and incremental dynamic analysis, Shock Vib. 17 (2010) 619–629, https://doi.org/10.3233/SAV-2010-0553.

[10] E. Kalkan, S.K. Kunnath, Assessment of current nonlinear static procedures for seismic evaluation of buildings, Eng. Struct. 29 (2007) 305–316, https://doi.org/10.1016/j.engstruct.2006.04.012.

[11] H. Krawinkler, G.D.P.K. Seneviratna, Pros and cons of a pushover analysis of seismic performance evaluation, Eng. Struct. 20 (1998) 452–464.

[12] M. Modirzadeh, S. Tesfamariam, A.S. Milani, Performance based earthquake evaluation of reinforced concrete buildings using design of experiments, Expert Syst. Appl. 39 (2012) 2919–2926, https://doi.org/10.1016/j.eswa.2011.08.153.

[13] O. Möller, R.O. Foschi, L.M. Quiroz, M. Rubinstein, Structural optimization for performance-based design in earthquake engineering: applications of neural networks, Struct. Saf. 31 (2009) 490–499, https://doi.org/10.1016/j.strusafe.2009.06.007.

[14] A. Mwafy, A. Elnashai, Static pushover versus dynamic collapse analysis of RC buildings, Eng. Struct. 23 (2001) 407–424, https://doi.org/10.1016/S0141-0296(00)00068-7.

[15] A. Neuenhofer, F.C. Filippou, Evaluation of nonlinear frame finite-element models, J. Struct. Eng. 123 (1997) 958–966, https://doi.org/10.1061/(ASCE)0733-9445(1997)123:7(958).

[16] D. Vamvatsikos, C.A. Cornell, Incremental dynamic analysis, Earthq. Eng. Struct. Dynam. 31 (2002) 491–514, https://doi.org/10.1002/eqe.141.

[17] M.D. Trifunac, Earthquake response spectra for performance based design—a critical review, Soil Dynam. Earthq. Eng. 37 (2012) 73–83, https://doi.org/10.1016/j.soildyn.2012.01.019.

[18] M. Mekki, S.M. Elachachi, D. Breysse, M. Zoutat, Seismic behavior of R.C. structures including soil-structure interaction and soil variability effects, Eng. Struct. 126 (2016) 15–26, https://doi.org/10.1016/j.engstruct.2016.07.034.

[19] R.A. Salgado, S. Guner, A comparative study on nonlinear models for performance-based earthquake engineering, Eng. Struct. 172 (2018) 382–391, https://doi.org/10.1016/j.engstruct.2018.06.034.

[20] M.R. Salami, M.M. Kashani, K. Goda, Influence of advanced structural modeling technique, mainshock-aftershock sequences, and ground-motion types on seismic fragility of low-rise RC structures, Soil Dynam. Earthq. Eng. 117 (2019) 263–279, https://doi.org/10.1016/j.soildyn.2018.10.036.

[21] J.J. Bommer, H. Crowley, The influence of ground-motion variability in earthquake loss modelling, Bull. Earthq. Eng. 4 (2006) 231–248, https://doi.org/10.1007/s10518-006-9008-z.

[22] D.M. Boore, Simulation of ground motion using the stochastic method, Pure Appl. Geophys. 160 (2003) 635–676, https://doi.org/10.1007/PL00012553.

[23] O.C. Celik, B.R. Ellingwood, Seismic risk assessment of gravity load designed reinforced concrete frames subjected to mid-America ground motions, J. Struct. Eng. 135 (2009) 414–424, https://doi.org/10.1061/(ASCE)0733-9445(2009)135:4(414).

[24] A.B. Liel, C.B. Haselton, G.G. Deierlein, J.W. Baker, Incorporating modeling uncertainties in the assessment of seismic collapse risk of buildings, Struct. Saf. 31 (2009) 197–211, https://doi.org/10.1016/j.strusafe.2008.06.002.

[25] O.-S. Kwon, A. Elnashai, The effect of material and ground motion uncertainty on the seismic vulnerability curves of RC structure, Eng. Struct. 28 (2006) 289–303, https://doi.org/10.1016/j.engstruct.2005.07.010.

[26] H. Aslani, E. Miranda, Probability-based seismic response analysis, Eng. Struct. 27 (2005) 1151–1163, https://doi.org/10.1016/j.engstruct.2005.02.015.

[27] N. Youssef, R. Wilkerson, K. Fischer, D. Tunick, Seismic performance of a 55-storey steel plate shear wall, Struct. Des. Tall Special Build. 19 (2009) 139–165, https://doi.org/10.1002/tal.545.

[28] A.R. Özuygur, Performance-based seismic design of an irregular tall building in Istanbul, Struct. Des. Tall Special Build. 24 (2015) 703–723, https://doi.org/10.1002/tal.1207.

[29] Y. Li, Y. Dong, D.M. Frangopol, D. Gautam, Long-term resilience and loss assessment of highway bridges under multiple natural hazards, Struct. Infrastruct. Eng. 16 (2020) 626–641, https://doi.org/10.1080/15732479.2019.1699936.

[30] N. Attary, V.U. Unnikrishnan, J.W. van de Lindt, D.T. Cox, A.R. Barbosa, Performance-Based Tsunami Engineering methodology for risk assessment of structures, Eng. Struct. 141 (2017) 676–686, https://doi.org/10.1016/j.engstruct.2017.03.071.

[31] M. Barbato, F. Petrini, M. Ciampoli, A preliminary proposal for a probabilistic performance-based hurricane engineering framework, Structures Congress 2011, American Society of Civil Engineers, Reston, VA, 2011, pp. 1618–1629, https://doi.org/10.1061/41171(401)141.

[32] A. Suksuwan, S.M.J. Spence, Performance-based multi-hazard topology optimization of wind and seismically excited structural systems, Eng. Struct. 172 (2018) 573–588, https://doi.org/10.1016/j.engstruct.2018.06.039.

[33] M.C. McCullough, A. Kareem, A framework for performance-based engineering in multi-hazard coastal environments, Structures Congress 2011, American Society of Civil Engineers, Reston, VA, 2011, pp. 1961–1972, https://doi.org/10.1061/41171(401)171.

[34] H. Tahir, R.T. Leon, M.M. Flint, Multi-Hazard Performance Based Design Multi-Hazard Performance Based Design, Virginia Polytechnic Institute and State University, 2016.
[35] N. Attary, J.W. Van De Lindt, A.R. Barbosa, D.T. Cox, V.U. Unnikrishnan, Performance-based tsunami engineering for risk assessment of structures subjected to multi-hazards: tsunami following earthquake, J. Earthq. Eng. (2019) 1–20, https://doi.org/10.1080/13632469.2019.1616335.
[36] G.Y.K. Chock, I. Robertson, H.R. Riggs, Tsunami structural design provisions for a new update of building codes and performance-based engineering, Solutions to Coastal Disasters 2011, American Society of Civil Engineers, Reston, VA, 2011, pp. 423–435, https://doi.org/10.1061/41185(417)38.
[37] I.N. Robertson, Development of performance based tsunami engineering (PBTE), advances and trends in structural engineering, mechanics and computation - proceedings of the 4th international conference on structural engineering, mechanics and computation, SEMC (2010) 161–164 2010, https://doi.org/10.2749/222137809796068091.
[38] N. Attary, J.W. van de Lindt, V.U. Unnikrishnan, A.R. Barbosa, D.T. Cox, Methodology for development of physics-based tsunami fragilities, J. Struct. Eng. 143 (2017) 04016223, https://doi.org/10.1061/(ASCE)ST.1943-541X.0001715.
[39] M. Ciampoli, F. Petrini, G. Augusti, Performance-based wind engineering: towards a general procedure, Struct. Saf. 33 (2011) 367–378, https://doi.org/10.1016/j.strusafe.2011.07.001.
[40] J.W. van de Lindt, T.N. Dao, Performance-based wind engineering for wood-frame buildings, J. Struct. Eng. 135 (2009) 169–177, https://doi.org/10.1061/(ASCE)0733-9445(2009)135:2(169).
[41] F. Petrini, M. Ciampoli, Performance-based wind design of tall buildings, Structure and Infrastructure Engineering 1–13 2011. https://doi.org/10.1080/15732479.2011.574815.
[42] M. Barbato, F. Petrini, V.U. Unnikrishnan, M. Ciampoli, Performance-based hurricane engineering (PBHE) framework, Struct. Saf. 45 (2013) 24–35, https://doi.org/10.1016/j.strusafe.2013.07.002.
[43] M. Khasreen, P.F.G. Banfill, G. Menzies, Life-cycle assessment and the environmental impact of buildings: a review, Sustainability 1 (2009) 674–701, https://doi.org/10.3390/su1030674.
[44] I. Zabalza Bribián, A. Valero Capilla, A. Aranda Usón, Life cycle assessment of building materials: comparative analysis of energy and environmental impacts and evaluation of the eco-efficiency improvement potential, Build. Environ. 46 (2011) 1133–1140, https://doi.org/10.1016/j.buildenv.2010.12.002.
[45] International Standards Organization (ISO), Environmental Management - Life Cycle Assessment - Principles and Framework, ISO 14040 Publication, 2006, p. 27.
[46] International Standards Organization (ISO), Environmental Management - Life Cycle Assessment - Requirements and Guidelines, ISO 14044 Publication, 2006, p. 8.
[47] R.A. Salgado, D. Apul, S. Guner, Life cycle assessment of seismic retrofit alternatives for reinforced concrete frame buildings, J. Build. Eng. 28 (2020) 101064, https://doi.org/10.1016/j.jobe.2019.101064.
[48] J.P.S. Chhabra, V. Hasik, M.M. Bilec, G.P. Warn, Probabilistic assessment of the life-cycle environmental performance and functional life of buildings due to seismic events, J. Architect. Eng. 24 (2018) 04017035, https://doi.org/10.1061/(asce)ae.1943-5568.0000284.
[49] G.A. Blengini, T. Di Carlo, The changing role of life cycle phases, subsystems and materials in the LCA of low energy buildings, Energy Build. 42 (2010) 869–880, https://doi.org/10.1016/j.enbuild.2009.12.009.
[50] I. Sartori, A.G. Hestnes, Energy use in the life cycle of conventional and low-energy buildings: a review article, Energy Build. 39 (2007) 249–257, https://doi.org/10.1016/j.enbuild.2006.07.001.
[51] C. Scheuer, G.A. Keoleian, P. Reppe, Life cycle energy and environmental performance of a new university building: modeling challenges and design implications, Energy Build. 35 (2003) 1049–1064, https://doi.org/10.1016/S0378-7788(03)00066-5.
[52] A. Peyroteo, M. Silva, S. Jalali, Life cycle assessment of steel and reinforced concrete structures: a new analysis tool, Portugal SB07. Sustainable Construction, Materials and Practices, 2007, pp. 397–402.
[53] X. Zhang, X. Su, Z. Huang, Comparison of LCA on steel- and concrete-construction office buildings: a case study, Sixth International Conference on Indoor Air Quality, Ventilation and Energy Conservation in Buildings: Sustainable Built Environment, 2006, p. 9.
[54] Å. Jönsson, T. Björklund, A.M. Tillman, LCA of concrete and steel building frames, Int. J. Life Cycle Assess. 3 (1998) 216–224, https://doi.org/10.1007/BF02977572.
[55] L. Lemay, Life Cycle Assessment of Concrete Buildings, National Ready Mixed Concrete Association (NRMCA), 2011, pp. 1–12.
[56] D. Peñaloza, J. Norén, P. Eriksson, Life Cycle Assessment of Different Building Systems: the Wälludden Case Study, Borås, Sweden, 2013.
[57] A.B. Robertson, F.C.F. Lam, R.J. Cole, A comparative cradle-to-gate life cycle assessment of mid-rise office building construction alternatives: laminated timber or reinforced concrete, Buildings 2 (2012) 245–270, https://doi.org/10.3390/buildings2030245.
[58] W. Peng, L. Sui Pheng, Managing the embodied carbon of precast concrete columns, J. Mater. Civ. Eng. 23 (2011) 1192–1199, https://doi.org/10.1061/(ASCE)MT.1943-5533.0000287.
[59] S. Saiz, C. Kennedy, B. Bass, K. Pressnail, Comparative life cycle assessment of standard and green roofs, Environ. Sci. Technol. 40 (2006) 4312–4316, https://doi.org/10.1021/es0517522.
[60] H.F. Castleton, V. Stovin, S.B.M. Beck, J.B. Davison, Green roofs: building energy savings and the potential for retrofit, Energy Build. 42 (2010) 1582–1591, https://doi.org/10.1016/j.enbuild.2010.05.004.
[61] A. Stephan, R.H. Crawford, K. de Myttenaere, A comprehensive assessment of the life cycle energy demand of passive houses, Appl. Energy 112 (2013) 23–34, https://doi.org/10.1016/j.apenergy.2013.05.076.
[62] S.M. Khoshnava, R. Rostami, R.M. Zin, D. Štreimikienė, A. Mardani, M. Ismail, The role of green building materials in reducing environmental and human health impacts, Int. J. Environ. Res. Publ. Health 17 (2020), https://doi.org/10.3390/ijerph17072589.
[63] B. Dong, C. Kennedy, K. Pressnail, Comparing life cycle implications of building retrofit and replacement options, Can. J. Civ. Eng. 32 (2005) 1051–1063, https://doi.org/10.1139/l05-061.
[64] Y. Dong, D.M. Frangopol, Performance-based seismic assessment of conventional and base-isolated steel buildings including environmental impact and resilience, Earthq. Eng. Struct. Dynam. 45 (2016) 739–756, https://doi.org/10.1002/eqe.2682.
[65] A. Belleri, A. Marini, Does seismic risk affect the environmental impact of existing buildings?, Energy Build. 110 (2016) 149–158, https://doi.org/10.1016/j.enbuild.2015.10.048.
[66] S. Proietti, P. Sdringola, U. Desideri, F. Zepparelli, F. Masciarelli, F. Castellani, Life Cycle Assessment of a passive house in a seismic temperate zone, Energy Build. 64 (2013) 463–472, https://doi.org/10.1016/j.enbuild.2013.05.013.
[67] T. Rodriguez-Nikl, Linking disaster resilience and sustainability, Civ. Eng. Environ. Syst. 32 (2015) 157–169, https://doi.org/10.1080/10286608.2015.1025386.
[68] M.V. Comber, C. Poland, M. Sinclair, Environmental impact seismic assessment: application of performance-based earthquake engineering methodologies to optimize environmental performance, Structures Congress 2012, American Society of Civil Engineers, Reston, VA, 2012, pp. 910–921, https://doi.org/10.1061/9780784412367.081.
[69] G.M. Calvi, L. Sousa, C. Ruggeri, Energy efficiency and seismic resilience: a common approach, in: P. Gardoni, J.M. LaFave (Eds.), Multi-Hazard Approaches to Civil Infrastructure Engineering, Springer International Publishing, Cham, 2016, pp. 165–208, https://doi.org/10.1007/978-3-319-29713-2_9.
[70] C.A. Feese, Assessment of Seismic Damage of Buildings and Related Environmental Impacts, Michigan Technological University, 2013.
[71] A. Hashemi, A. Valadbeigi, R. Masoudnia, P. Quenneville, Seismic resistant cross laminated timber structures using an innovative resilient friction damping system, Proceedings of the 2016 New Zealand Society of Earthquake Engineering Conference (NZSEE), Christchurch, New Zealand, 2016, p. 8.
[72] H.-H. Wei, M.J. Skibniewski, I.M. Shohet, X. Yao, Lifecycle environmental performance of natural-hazard mitigation for buildings, J. Perform. Constr. Facil. 30 (2016) 04015042, https://doi.org/10.1061/(asce)cf.1943-5509.0000803.
[73] K.L. Sibanda, S. Kaewunruen, Life cycle assessment of retrofit strategies applied to concrete infrastructure at railway stations exposed to future extreme events, in: A. Ivankovi, M. Mari, A. Strauss, T. Kišiek (Eds.), International Conference on Sustainable Materials, Systems and Structures (SMSS 2019): Challenges in Design and Management of Structures, vol. 4, RILEM Publications S.A.R.L., Rovinj, Croatia, 2019, pp. 168–175.
[74] S. Marinković, V. Radonjanin, M. Malešev, I. Ignjatović, Comparative environmental assessment of natural and recycled aggregate concrete, Waste Manag. 30 (2010) 2255–2264, https://doi.org/10.1016/j.wasman.2010.04.012.
[75] G.A. Blengini, Life cycle of buildings, demolition and recycling potential: a case study in Turin, Italy, Build. Environ. 44 (2009) 319–330, https://doi.org/10.1016/j.buildenv.2008.03.007.
[76] Federal Emergency Management Agency (FEMA), Next-Generation Performance-Based Seismic Design Guidelines, Federal Emergency Management Agency, Washington, D.C., 2006.
[77] H. Krawinkler, Van Nuys Hotel Building Testbed Report: Exercising Seismic Performance Assessment, Berkeley, 2005.
[78] Federal Emergency Management Agency (FEMA), NEHRP Commentary on the Guidelines for the Seismic Rehabilitation of Buildings, FEMA 274 Publication, 1997, p. 488.
[79] Applied Technology Council, Guidelines for nonlinear structural analysis and design of buildings. Part I - general, NIST GCR 17-917-46v1 Publication 137 2017. https://doi.org/10.6028/NIST.GCR.17-917-46v1.
[80] S.W. Han, A.K. Chopra, Approximate incremental dynamic analysis using the modal pushover analysis procedure, Earthq. Eng. Struct. Dynam. 35 (2006) 1853–1873, https://doi.org/10.1002/eqe.605.
[81] American Society of Civil Engineers (ASCE), Seismic evaluation and retrofit of existing buildings, ASCE 41 publication 576 2017. https://doi.org/10.1061/9780784414859.
[82] American Society of Civil Engineers (ASCE), Seismic Rehabilitation of Existing Buildings, American Society of Civil Engineers, Reston, VA, 2007.
[83] Federal Emergency Management Agency (FEMA), Seismic Performance Assessment of Buildings. Volume 4 - Methodology for Assessing Environmental Impacts, FEMA P-58-4 Publication, 2018, p. 122.
[84] K.A. Hossain, B. Gencturk, Life-cycle environmental impact assessment of reinforced concrete buildings subjected to natural hazards, J. Architect. Eng. 22 (2016) A4014001, https://doi.org/10.1061/(ASCE)AE.1943-5568.0000153.
[85] A. Ceccotti, C. Sandhaas, M. Okabe, M. Yasumura, C. Minowa, N. Kawai, SOFIE project - 3D shaking table test on a seven-storey full-scale cross-laminated timber building, Earthq. Eng. Struct. Dynam. 42 (2013) 2003–2021, https://doi.org/10.1002/eqe.2309.
[86] European Committee for Standardization (CEN), Eurocode 8: Design of Structures for Earthquake Resistance - Part 1: General Rules, Seismic Actions and Rules for Buildings, EN 1998-1:2004 Publication, 2004, p. 229.
[87] C. Petrone, T. Rossetto, K. Goda, Fragility assessment of a RC structure under tsunami actions via nonlinear static and dynamic analyses, Eng. Struct. 136 (2017) 36–53, https://doi.org/10.1016/j.engstruct.2017.01.013.

[88] American Society of Civil Engineers (ASCE), Minimum Design Loads and Associated Criteria for Buildings and Other Structures, ASCE 7 Publication, 2017, p. 889.
[89] Z.X. Qi, I. Eames, E.R. Johnson, Force acting on a square cylinder fixed in a free-surface channel flow, J. Fluid Mech. 756 (2014) 716–727, https://doi.org/10.1017/jfm.2014.455.
[90] National Concrete Masonry Association, Design of concrete masonry infill, 2019. https://ncma.org/resource/design-of-concrete-masonry-infill/. (Accessed 5 July 2020).
[91] N. Attary, J.W. van de Lindt, V.U. Unnikrishnan, A.R. Barbosa, D.T. Cox, Methodology for development of physics-based tsunami fragilities, J. Struct. Eng. 143 (2016) 12, https://doi.org/10.1061/(ASCE)ST.1943-541X.0001715.
[92] J. Bare, TRACI 2.0: the tool for the reduction and assessment of chemical and other environmental impacts 2.0, Clean Technol. Environ. Policy 13 (2011) 687–696, https://doi.org/10.1007/s10098-010-0338-9.
[93] Sphera, GaBi ts - life cycle assessment software, 2020. http://www.gabi-software.com/america/index/.
[94] H. Guo, Y. Liu, Y. Meng, H. Huang, C. Sun, Y. Shao, A comparison of the energy saving and carbon reduction performance between reinforced concrete and cross-laminated timber structures in residential buildings in the severe cold region of China, Sustainability 9 (2017) 1426, https://doi.org/10.3390/su9081426.
[95] H.J. Darby, A.a. Elmualim, F. Kelly, A case study to investigate the life cycle carbon emissions and carbon storage capacity of a cross laminated timber, multi-storey residential building, Proceedings of the World Sustainable Building Conference, Singapore, 2013, pp. 1–8.
[96] A. Hafner, S. Schäfer, Comparative LCA study of different timber and mineral buildings and calculation method for substitution factors on building level, J. Clean. Prod. 167 (2017) 630–642, https://doi.org/10.1016/j.jclepro.2017.08.203.
[97] J.L. Skullestad, R.A. Bohne, J. Lohne, High-Rise timber buildings as a climate change mitigation measure – a comparative LCA of structural system Alternatives, Energy Procedia 96 (2016) 112–123, https://doi.org/10.1016/j.egypro.2016.09.112.
[98] C. Chen, F. Pierobon, I. Ganguly, Life cycle assessment (LCA) of cross-laminated timber (CLT) produced in western Washington: the role of logistics and wood species mix, Sustainability 11 (2019) 1278, https://doi.org/10.3390/su11051278.